International Journal on Advanced Science Engineering Information Technology

Vol.12 (2022) No. 1
ISSN: 2088-5334

Moving Quick Response Codes Identification: System Performance Analysis and Maximization by Optimization of Illuminance and Exposure Time

Muhammad S. Y. Sunarko [a], Faridah [a,*], Agus Arif [a], Balza Achmad [a]

[a] *Department of Nuclear Engineering and Engineering Physics, Universitas Gadjah Mada, Yogyakarta, Indonesia*
Corresponding author: [*]faridah@ugm.ac.id

***Abstract*— We studied the relationship of Quick Response (QR) code identification system performances with illuminance on the QR code, exposure time of the camera, and relative moving speed. We studied the root causes of low identification performance problems on moving QR code as well. A physical experiment method study on a minimal working example of a real-time moving QR codes identification system with ZBar QR codes identification algorithm has done, and then the results were quantitatively and qualitatively analyzed. The values of illuminance on the QR code, exposure time of the camera, and relative moving speed used in the experiments were 140 lux - 640 lux, 0.7 ms - 22.2 ms, and 0 m/s - 2.5 m/s, respectively. Our data boundaries of the experiment results regarding exposure and motion blur (mediator variables) were respectively 0.108 lux·s - 12.476 lux·s and 0.0 pixel - 30.4 pixel. We identified physical phenomena in imaging, exposure and motion blur, could make the QR code image too dark/too bright and motion blurred. Such phenomena could make the QR code hard to identify and being the root cause of the problems. Our quantitative study proved that identification system performance is affected by illuminance, exposure time, and relative moving speed. Finally, we proposed a novel solution to overcome the problems by using a numerical method to compute the optimal illuminance on the QR code and the camera's exposure time for the given relative moving speed of the system.**

***Keywords*— Quick Response code; identification performance; moving speed; exposure; illuminance; optimization.**

Manuscript received 17 Aug. 2020; revised 25 Feb. 2021; accepted 15 Mar. 2021. Date of publication 28 Feb. 2022.

I. INTRODUCTION

Quick Response (QR) codes are widely used by various applications which require reliable QR codes identification, such as mobile robot localization and navigation [1]–[4], transportation platform localization and navigation [5], [6], augmented reality [7], smart wheelchair localization and navigation [8], real-time objects identification for the visually impaired [9], structural displacement measurement [10], conveyer belt in the agro-food supply chain [11], [12], warehouse management [13], autonomous library robot [14], indoor parking vehicle-tracking system [15], and high-speed moving cars identification [16]. Many researchers developed novel QR codes identification algorithms and QR codes identification algorithms enhancements to achieve maximum identification performance.

For example, Brown [17] developed an open-source library named ZBar to identify various barcodes symbols, including QR codes, by making linear scans pass over an image. Szentandrási *et al.* [18] implemented a Histogram of Gradients to locate QR codes from an image, identifying success rate at about 73.3%, in upright QR codes, rotated QR codes, and irregular illumination conditions. Szentandrási *et al.* [18] also reported that ZBar had an average identification success rate of about 78.3% for the same conditions.

Liu *et al.* [19] integrated global thresholding with local thresholding in an image binarization process. The recognition rate in normal lighting conditions was 97.5%, highlighted spot and background noise was 95%, low contrast or non-homogeneous lighting was 91%, and damaged bar code was 87%. He and Yang [20] proposed adaptive local binarization based on sets of threshold rules and adaptive window size for different illumination conditions to improve ZBar recognition rate on non-homogeneous illumination from 94.41% to 95.65%. Hogpracha and Vongpradhip [16] used the contrast limited adaptive histogram equalization before converting a binary image for moving QR codes identification. The identification success rates of QR codes attached on moving cars were about 100% for under 8.33 m/s, 80% at 9.72

m/s, and 60% at 11.11 m/s. Pu *et al.* [21] proposed a Convolutional Neural Network-based framework for image pre-processing on QR codes identification using ZBar to recover blurry QR codes caused by out-of-focus blur and motion blur. Yu [22] proposed a method to do image deblurring using fractional differential order. Both Pu *et al.* [21] and Yu [23] were able to reach the QR codes recognition rate >90%.

QR codes identification algorithms and its enhancements are widely developed to achieve maximum identification performance and reliable identification systems. The root causes of low identification performances were still unclear. Jahr [24] stated that lighting in machine vision has many parameters and complex relationships that affect image processing algorithms' performance in general. Jahr [24] used illuminance as a quantitative lighting measurement on reflective objects. Ye *et al.* [10] and Zhang *et al.* [1] adjusted the camera's exposure time/shutter speed to adapt to the lighting condition, but this is not yet explained or analyzed quantitatively. Qian *et al.* [11] analyzed the relationship of QR code readability with reading distance, code size, coded characters, and moving speed factors, but lighting and imaging device factors were not discussed.

This study examined the relationship between QR code identification system performances and illuminance E on the QR code, camera exposure time t, and relative moving speed v. A study case on a minimal working example of real-time moving QR codes identification system with ZBar algorithm has done. The results were quantitatively and qualitatively analyzed. Recall r and precision p used as the QR codes identification system [25]. The root causes of low identification system performance problems on moving QR code were studied as well. We identified that physical phenomena in imaging (i.e., exposure and motion blur) could make the QR code image too dark/too bright and motion blurred. Such phenomena could make the QR code hard to identify and being the root cause of the problems. Our study quantitatively proved that varying E, t, and v affects the identification system performances. Finally, we propose a novel solution to overcome the problems by using a numerical method to compute the optimal E on the QR code and t of the camera for a given v of the system.

II. Material and Method

A. Related Works

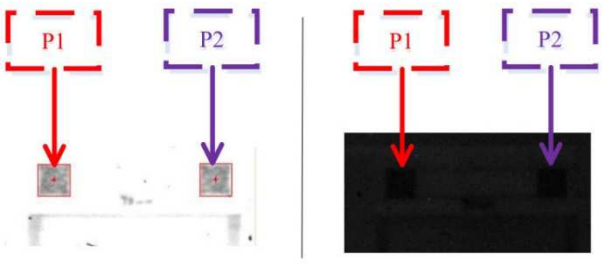

Fig. 1 QR code images respectively at illuminance of 600 lux and 75 lux [10]

Ye *et al.* [10] investigated the error sources on the measurement accuracy on a non-contact vision-based structural displacement measurement system. The purpose of the investigation was to achieve accurate and reliable measurement by making effective measures against various error sources: environmental illumination, the elevation angle of the digital camera, and the vapor surrounding the targets. The environmental illumination was quantitatively measured using illuminance on the object. However, the measurement results were only descriptively analyzed. The QR codes were grayish, and the region around the QR codes was bright in the image at the illuminance of 600 lux. The QR codes were stand out from the surrounding environment, and the QR codes were successfully detected. At the illuminance of 75 lux, the QR codes were tough to be detected because the QR codes and the region around them were almost integrated. Fig. 1 shows both of the images at the illuminance of 600 lux and 75 lux. The investigation result concluded that the illumination on the object affected the resulting images and affected the success of QR codes detection.

Zhang *et al.* [1] adjusted the camera's exposure time to adapt to the lighting condition. However, it was unclear how Zhang *et al.* [1] set the camera's exposure time and how much the illuminance for the object needed. Hogpracha and Vongpradhip [16] showed that moving speed affected the QR code identification success rate, but it still has not yet been explained why and how it happened.

B. Methodology

We used the experimental method to investigate the system's identification performances against various illuminance, exposure time, and moving speeds. A system identified QR codes, and then the results were saved to estimate the quantitative identification performance using recall and precision. The relationships of recall and precision with illuminance, exposure time, and moving speed were searched using regression. Illuminance and exposure time of the identification system relative to QR codes moving speeds optimized using numerical method. We did our research in several stages, as described in Fig. 2.

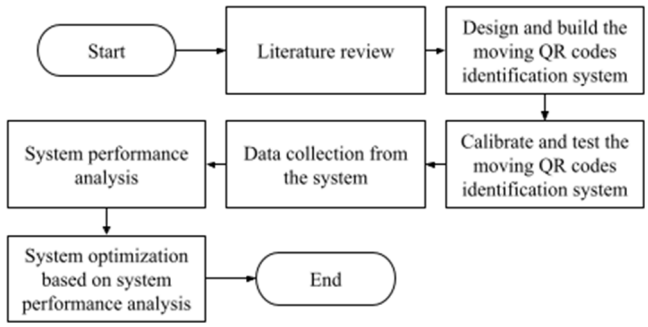

Fig. 2 Stages of our research

1) Moving QR Codes Identification System: The identification system consisted of an electronic global shutter camera, a camera lens, homogeneous light sources, a processing device/personal computer (PC), and software with a QR code identification algorithm. An electronic global shutter camera was used instead of an electronic rolling shutter camera; because of the scanning on the electronic rolling shutter imaging sensor, Mattfeldt [26] might cause the object to be skewed when the object is moving fast. The camera had manual control of exposure time, gain, and white balance. The manual control of gain was used to ensure that the gain was always at the default value and remain

unchanged during camera usage. The white balance of the image should be adjusted so that the white objects appeared white on the resulting image. Incorrect setting of the white balance may cause color inconsistencies in the image [27].

We determined the size of the QR code and the focal length of the camera lens by taking a preliminary test. The purpose of the preliminary test was to assure that the system could identify the QR code in a static condition and d_{ob} at 1.5 m. The condition was defined as static v = 0 m/s, and the resulting image had qualitatively adequate lighting. The definition of qualitatively adequate lighting was that humans could see the QR codes clearly in the image. In our experiment, qualitatively adequate lighting was achieved when the illuminance on the QR codes was 40.5 lux, and the camera's exposure time was 12.5 ms. The f_{lens} determine the imaging system's angle of view (AOV) and the field of view (FOV). The AOV could be calculated with[28]

$$AOV_s = 2\,arctan\left(\frac{s_{sensor}}{2f_{lens}}\right). \quad (1)$$

To accurately determines the FOV of the imaging system, we directly measured the side length of a flat object plane captured by the imaging system using a ruler. The camera had placed at the distance d_{ob} from the object plane before the FOV measured. The d_{ob} on FOV measurement was the same as the distance of the camera to the QR codes.

Lighting technique of partial bright field incident light, Jahr [24] used to illuminate the QR codes. Homogeneous or defined, known and repeatable brightness profile was one of the requirements for the lighting in machine vision [24], so we preferred to follow it in our experiment and recommend it for other machine vision applications. A lux light meter used to measure the illuminance at the QR code surface. If the distance between the light sources and the QR codes were constant, then the illuminance could be measured only once as long as the lighting did not decay significantly within a specified period (known and repeatable brightness profile criterion).

This paper only discussed reflecting/incident light QR codes (e.g., QR codes printed on a surface). Glowing/backlight QR codes (e.g., QR codes displayed on a liquid crystal display) were not discussed and are irrelevant to this paper's discussion. The QR code should contain the data to be identified by the QR codes identification system. For a fair identification performance result, the rotation of the QR codes should be considered [18]. An assumption is that QR codes have uniformly distributed random rotations from 0° to 360° applied. A speed measurement device was used to measure the relative moving speed if there was relative movement between QR codes and the identification system, whether the QR codes itself were moving or the identification system was moving. If there was no relative movement, then it could be assumed that $v$it was 0 m/s.

2) System performance analysis: Many performance metrics were available for evaluating QR codes identification systems [25]. The QR codes identification results counted as one of four categories. If a QR code is present and correctly identified, then it counted as TP. If a QR code is present and the identification failed, then it counted as FN. If no QR code, but the identification result is giving that a QR code present (i.e., false alarm), it counted as FP. If no QR code and the identification result give no QR code present, it counted as TN. TN was irrelevant for QR codes identification systems with QR codes area and position estimations within the image frame. Every single pixel that is no QR code and not identified as QR code was a TN so that the TN count would be incorrect. Recall is defined by Godil *et al* [25] as follows:

$$r = \frac{TP}{TP+FN} \quad (2)$$

The recall is the fraction of correctly detected items among all the items that should be detected. Precision is defined by Godil *et al.* [25] as

$$p = \frac{TP}{TP+FP} \quad (3)$$

Precision is the fraction of detected items that are correct. Recall and precision are used as performance metrics for evaluating QR codes identification systems.

There was illuminance, exposure time, and moving speed as independent variables, while recall and precision were dependent variables. The relationship of recall with independent variables and precision with independent variables were searched using regression analysis. The independent variables were approached by using exposure and motion blur as mediator variables based on Jahr [24] that simplified the regression analysis and explained the physical phenomena during QR codes identification with various values of independent variables.

Fig. 3 Example images from the experiment at v=0 m/s with proper (E=294 lux, t=5.6 ms, recall=76.05%), over-exposed (E=556 lux, t=22.2 ms, recall=0.00%), and under-exposed (E=165 lux, t=0.7 ms, recall=0.00%) exposure

Exposure is defined by Jahr [24] as follows:

$$H = E \cdot t. \quad (4)$$

In general, the main goal was to produce images with sufficient contrast (light and dark), not over-exposed and not under-exposed, as illustrated in Fig. 3. QR codes identification could fail if the image's QR codes did not have sufficient contrast because the image was over-exposed or under-exposed (as seen in Fig. 3).

Motion blur is defined by Jahr [24] as

$$MB = v \cdot t \cdot \frac{n_m}{FOV_m}. \quad (5)$$

In general, the main goal was to produce images with the lowest motion blur. However, since relative moving speed is a requirement in many applications, the relative moving speed could not decrease the motion blur. Decreasing exposure time could reduce motion blur, but it would change the exposure. Increasing the illuminance could compensate for the decrement of the exposure time so that the exposure did not change.

Maximum recall and precision hypothetically expected if exposure and motion blur were at an optimum value. If the

relationships between dependent variables and mediator variables are already known, then the relationships between dependent variables and independent variables could be easily obtained by substitutions with Equation 4 and Equation 5. The optimization process could use the known relationship of QR codes identification performance with illuminance, exposure time, and moving speed.

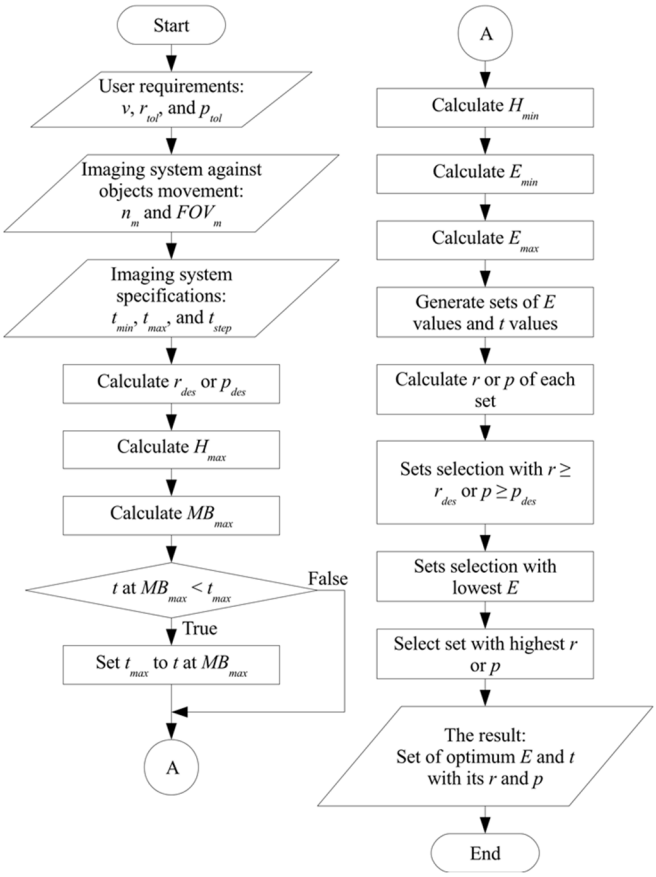

Fig. 4 Illuminance and exposure time optimization on QR codes identification systems

3) Illuminance and exposure time optimization: We varied exposure time and illuminance to calculate a set of various recall and precision of the QR codes identification systems for a particular moving speed. Our calculations were valid only within our data boundaries of the experiment results in terms of exposure and motion blur. The optimum illuminance and exposure time were obtained from the set with recall and precision that fulfilling the required minimum values. Fig. 4 shows the flowchart of illuminance and exposure time optimization on QR codes identification systems to achieve maximum identification systems performance. The relative moving speed of the system against the QR codes should be specified, and it could be a single value or a range of values. The moving direction should be specified first to specify the camera sensor's pixel count in the moving direction of the objects n_m and the FOV in the moving direction of the objects FOV_m. Minimum exposure time t_{min}, maximum exposure time t_{max}, and the step of exposure time t_{step} known from the camera specifications.

The desired chosen performance metric, which was relatively lower from the maximum possible chosen performance metric (i.e., r_{tol} or p_{tol}), was calculated as the desired chosen performance metric (i.e., r_{des} or p_{des}) using

$$r_{des} = r(1 - r_{tol})_{max} \quad (6)$$

or

$$p_{des} = p(1 - p_{tol})_{max} \quad (7)$$

where r_{max} and p_{max} were the maximum possible values of recall and precision. The desired performance metric was specified as relative values to avoid specifying more than the maximum possible value. Values of r_{tol} or p_{tol} given with low value (e.g., 0.1%) for a result close to the maximum possible value of the performance metric. However, it should not 0 to avoid excessive illuminance requirements with an insignificant increase in the performance metric. If the intention is for drawing charts, we used higher values (e.g., 5%) of r_{tol} or p_{tol} to wider the charts coverage range.

The r_{max} or p_{max} obtained from the maximum point of the regression equations of the performance metric (i.e., recall or precision) against H at no motion blur (MB = 0 pixel), i.e., v = 0 m/s. The upper boundary of the exposure (H_{max}) was the value of H where the r_{max} or p_{max} located. The upper boundary of the motion blur (MB_{max}) was obtained using the inverse of the regression equations of the performance metric (i.e., recall or precision) against exposure and motion blur, with Hmax used for the value of the exposure giving r_{des} to that inverse.

The t at MB_{max} calculated as follows. If the t at MB_{max} is less than specified t_{max}, then the value of the t_{max} was replaced with the value of the t at MB_{max}. The purpose of this step was to reduce sets of unnecessary E and t values with the low value of the performance metric (i.e., recall or precision) because of high t value (hence MB was greater than MB_{max}). The lower boundary of the exposure (H_{min}) obtained by using the inverse of the regression equations of the performance metric (i.e., recall or precision) against exposure with no motion blur, then giving r_{des} to that inverse. H_{min} and H_{max} could be given to Equation 4 so that the lower and upper boundary of the illuminance (E_{min} and E_{max}) were obtained, respectively.

We generated sets of E and t values for given v within boundaries that had already been obtained before. The recall and precision value for each of the generated E and t value set calculated using the regression equation of the recall and precision against E, t, and v. Charts could be drawn from the generated E and t values for given v with its recall and precision values set.

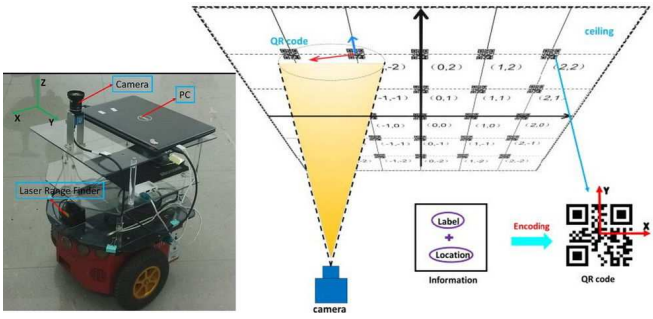

Fig. 5 Mobile robot and QR codes used in the system proposed by [1], respectively

Sets with recall or precision higher than the desired ones were selected. By now, the sets may contain several sets that

had nearly the same performance metric value that was focused on being maximized but with different E and t values. Therefore, sets with the lowest E were selected to reduce the required illuminance (hence the required electric power). The set with the highest focused performance metric value within the lowest E is then selected, so that set with the optimum E and t for a given v with maximum QR codes identification performance obtained. The obtained set of values used and suggested for designing the QR codes identification system.

*4) A study case on the ZBar algorithm: The study case of the QR codes identification system i*s done by approaching the localization and navigation system using the QR code for a mobile robot in an indoor environment. We used the system proposed by Zhang *et al.* [1] (as seen in Fig. 5) using the ZBar algorithm for QR code identification as the reference for our approach, so we tried to mimic their QR code identification system configuration. The mobile robot is considered as a platform that made the QR codes identifications system move with measurable constant speeds. So, the mobile robot could be replaced with any moving object (or even the QR codes is moving instead) as long as the moving speed could be measured and constant.

The QR codes version 2 used for the experiment in this paper contained 12 alphanumeric characters data with the template "(NN, X.X,Y.Y)" (without quotation marks). "NN" was two digits QR code numbering, "X.X" and "Y. Y" were decimal coordinates within the x-axis and the y-axis. The error correction level set to the highest available level, i.e., level H (~30% per symbol area) [29]. The QR codes were placed at the ceiling of the 2nd-floor corridor of the Department of Nuclear Engineering and Engineering Physics, Universitas Gadjah Mada (DTNTF FT-UGM) building, as seen in Fig. 6.

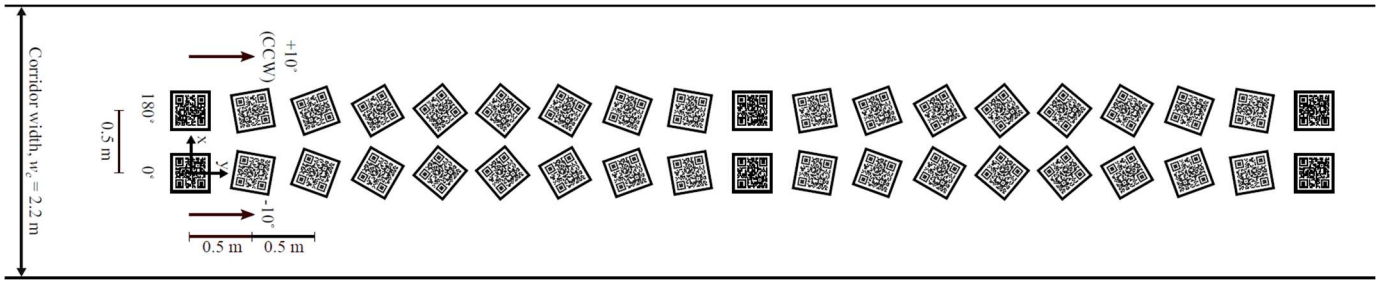

Fig. 6 QR codes placement layout at the ceiling of 2nd-floor corridor DTNTF FT-UGM building

The QR codes were printed in 12 cm × 12 cm size each and spaced 0.5 m from each other. The purpose of the rotations of QR codes placement was to assume that the camera could capture any QR code image with any rotation (0°–360°); each QR code rotation has the same probability.

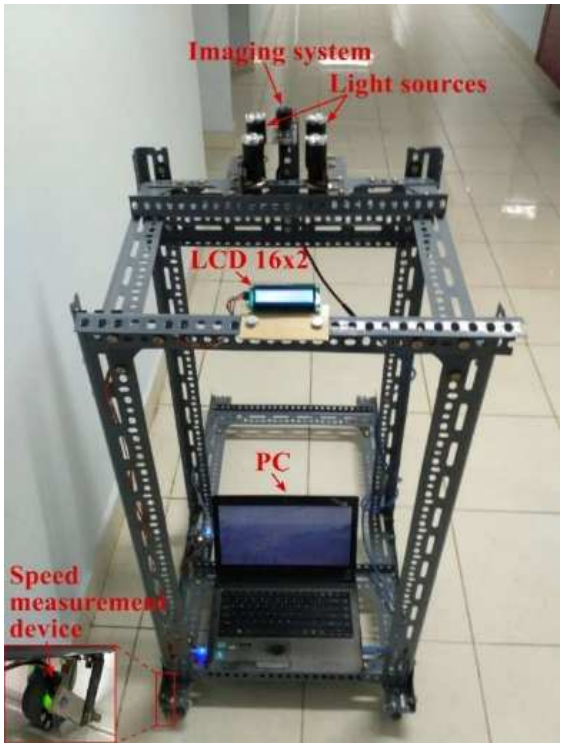

Fig. 7 Platform mobile robot prototype

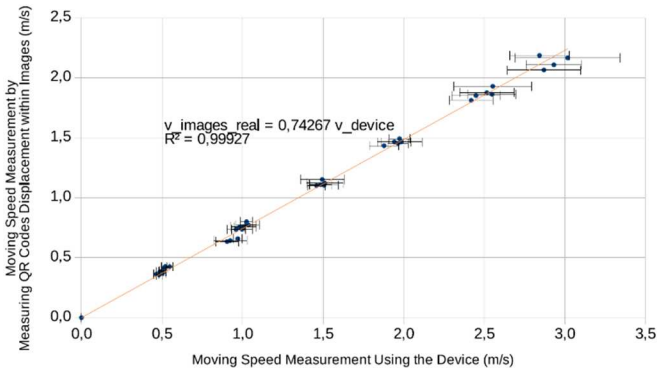

Fig. 8 The result of speed measurement device calibration

In this paper, a trolley-like made of thick slotted angle bars and rubber wheels (as shown in Fig. 7) used, performing as the platform mobile robot prototype. A reflective infrared transceiver CNY 70 module, a reflective printed incremental rotary encoder, an Arduino Leonardo, and a Liquid Crystal Display (LCD) 16×2 used to construct a speed measurement device. We used the period measurement method for speed measurement [30]. The device was calibrated with a moving speed measurement by measuring QR codes displacements within images, as the distances between QR codes were fixed and well-known. The prototype moved by driving it manually with constant walking speed, keeping the moving speed shown in the LCD as near as possible to the target moving speed. The moving speed was real-time measured and recorded with a minimum sampling rate of 28.7 Hz at 0.25 m/s, and this rate was increasing as the moving speed increases. The device calibration result (as seen in Fig. 8)

shows that each average moving speed has a relatively small standard deviation to the average value, showing that the prototype moved with constant speed. The measurement error was getting higher as the moving speed was getting higher; this was true because the device's measurement method was only optimized for low-speed measurement [30]. Higher prototype moving speed also getting more challenging to drive manually at a constant speed, so the moving speed for the experiment in this paper was limited up to 2.5 m/s.

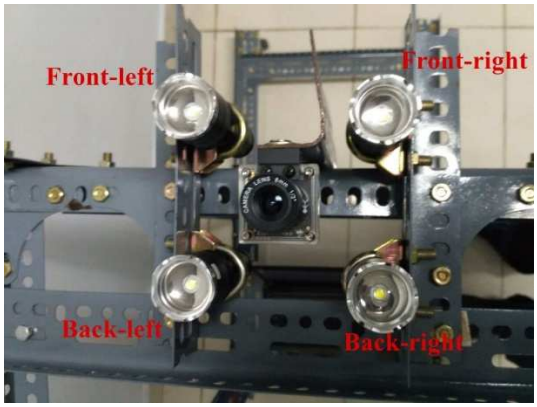

Fig. 9 The LEDs used as the light sources

Our imaging system configuration consisted of a high frame rate oCam 1CGN-U electronic global shutter camera, and a camera lens. The camera placed on the prototype with a distance from the ceiling d_{ob} of 1.5 m. The camera had an AR0134CS CMOS 1/3 inch format imaging sensor with an image resolution of 1280 pixels × 960 pixels, having $s_{diagonal\ sensor}$ of 6.0 mm, horizontal $s_{horizontal\ sensor}$ of 4.8 mm, and $s_{vertical\ sensor}$ of 3.6 mm. The red white balance (WB) of the camera set to 133 and blue WB set to 125. The gain control set to manual with a default value of 64. The camera had a minimum exposure time t_{min} of 0.1 ms, and the exposure time step t_{step} was 0.1 ms. The maximum exposure time t_{max} was the inverse of the camera's maximum frame rate (i.e., 45 frames per second) so that it was 22.2 ms. The camera's maximum frame rate limited by the pixel clock rate and related circuitry in the camera and how fast it can put images onto a camera bus [27]. The frame rate and the camera's exposure time had separate controls, so it was possible to set the exposure time, e.g., to 5.6 ms, while maintaining the frame rate at 45 frames per second. Since the frame rate was not related to the exposure time and was only related to the data transfer rate, the frame rate had no relation with QR code identification performance (recall in this case). Frame rate had the only relation with images sampling rate, i.e., 45 images per second.

A camera lens with focal length f_{lens} of 8 mm and an aperture number f/1.2 was used for the camera, having $FOV_{diagonal}$ of 1.18 m, $FOV_{horizontal}$ of 0.95 m, and $FOV_{vertical}$ of 0.70 m. The ratio between the side length of the QR code and the $FOV_{vertical}$ was 0.17143. We did not address the light sensitivity of our imaging system configuration since we did not have access to the measurement device. The values in our results are only valid for the same imaging system configuration, but our approach is general for all imaging system configurations.

There were four units of zoom LED XM-L2 used as the light sources, placed at the side of the imaging device at 6.5 cm, as seen in Fig. 9. The light sources had an angular distance to the imaging device at about 4.96°. The light sources had 2.2 m diameter circle lighting area. So, we had partially directed bright field incident light as the lighting technique. The experiments had been done in night conditions so that the illuminance on the QR codes from the environment was very low, only about 2–3 lux. A standard lux light meter Extech 401025 was used to measure the illuminances. Table 1 shows illuminance on each QR code where the light sources were at the center between four QR codes (two rows and two columns) and the light sources turned on alternately. Each LED had a relatively small illuminance difference on each QR code position. Each LED had a relatively small illuminance standard deviation (S.D.) to its average. So, each LED assumed as a homogeneous light source. Batteries supplied the powers for the LEDs, and their illuminances were decaying over turned-on time. So, an illuminance measurement from some turned-on LEDs (depending on experiment set) performed for each experiment beginning.

TABLE I
LEDs HOMOGENEITY TEST

LED	Illuminance (lux) on QR Code No.				Average	S.D.
	1	20	2	21		
Back-left	144	139	137	145	141.25	3.86
Back-right	142	150	135	145	143.00	6.27
Front-left	148	145	160	159	153.00	7.62
Front-right	132	133	152	150	141.75	10.72

A laptop (PC) with Intel Core i7-2640QM processor, an 8 GB RAM, and a 5400-rpm hard disk drive (HDD) used for the real-time QR codes identification system. The QR codes identification software made using C++ language, and OpenCV with the QR codes identification algorithm was ZBar open-source library. The software functions were: to capture images from the camera, to read the moving speed measurement device, to receive inputs (i.e., measured illuminance, target moving speed, and exposure time setting), to get a real-time QR codes identification, to save identification results as an image format (JPG), and to save all parameters value with the text version of identification results as comma-separated value (CSV) text format. The average overall required time to identify QR codes within an image was 62.02±4.96 ms, so that the QR codes' identification frequency was about 16.12 images per second.

III. Results and Discussion

A. The system's performance

All the independent variables were varied for each experiment set in this paper. The exposure time values were 22.2 ms, 10.5 ms, 5.6 ms, 2.7 ms, 1.3 ms, and 0.7 ms. For the desired moving speed, the values were 0 m/s, 0.25 m/s, 0.5 m/s, 0.75 m/s, 1 m/s, 1.5 m/s, 2 m/s, and 2.5 m/s on vertical direction of the imaging system. The values for the illuminance varied by changing the amount of the turned-on LEDs, i.e., 1 LED, 2 LEDs, 3 LEDs, and 4 LEDs with illuminance value at about 140 lux - 200 lux, 260 lux - 340 lux, 370 lux - 500 lux, and 520 lux - 640 lux, respectively.

The data acquisition for each set of the experiment done three times to ensure the validity of the data; all three data

acquisitions used and shown separately. We were not doing higher moving speed experiment sets that had recall precisely 0 for the same illuminance and exposure time. Such experiment sets would have higher motion blurs, and the identification performances would not be better. Our data boundaries of the experiment results in terms of exposure and motion blur (mediator variables) were respectively 0.108 lux·s - 12.476 lux·s and 0.0 pixel - 30.4 pixel.

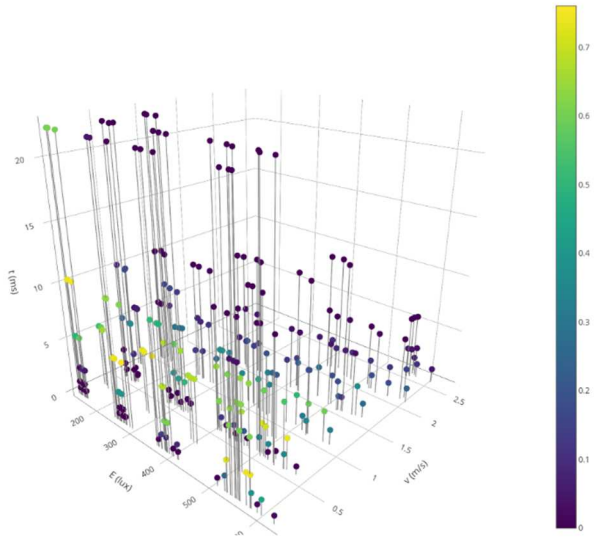

Fig. 10 Recall of QR codes identification system with ZBar algorithm against illuminance, exposure time, and moving speed

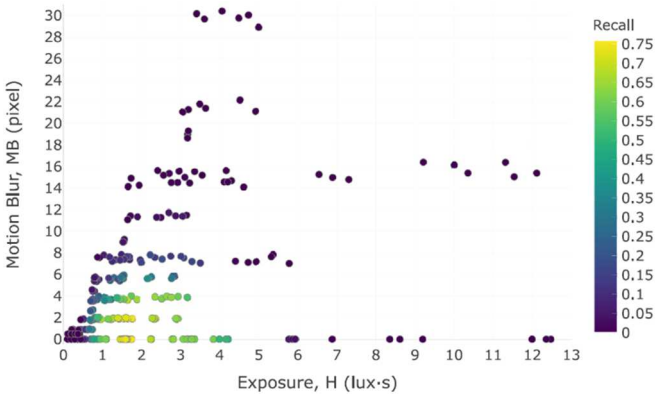

Fig. 11 Recall of QR codes identification system with ZBar algorithm against exposure and motion blur

We compared image format data with the text format data to categorize whether a QR code was a TP, an FP, or an FN; then, we summed each of them in an experiment set. We calculated recall and precision for an experiment set; both represent the QR codes identification systems performance. We got the system's precision for each experiment set was always 100% because there was no FP at all. That was true because the QR codes were structured well enough, and the algorithm itself was optimized to suppress FP/false alarms, as stated in the comments of ZBar source codes. Fig. 10 shows recall of the system against illuminance, exposure time, and moving speed.

The recalls for certain moving speeds were only high if the illuminance and exposure time is at optimum value. We introduced mediator variables: exposure and motion blur to better explain the physical phenomena affecting the systems recall. The QR codes identification systems performance (as seen in Fig. 11) was deficient if the exposure value was too low or too high. That was true because the contrast of the QR codes reduced when the images were under-exposed or over-exposed so that the QR codes identification failed. The QR codes also failed to be identified if the motion blur was too high. That was true because the QR codes structure in the images was blurred, distorted, and overlapping each other, as seen in Fig. 12.

Fig. 12 QR code images respectively at exposure value *H* 2.76, 3.18, 1.05, and 2.76 lux·s, motion blur *MB* 3.8, 3.8, 3.8, and 14.5 pixels, and recall 63.26%, 54.29%, 31.25%, and 0.61%

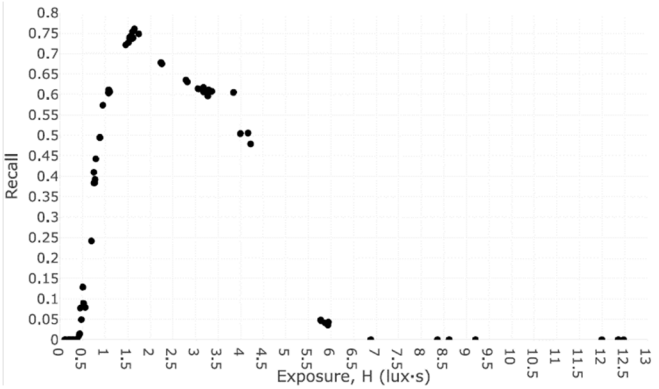

Fig. 13 Recall of QR codes identification system with ZBar algorithm against exposure with no motion blur

The QR codes identification system had a maximum recall of 76.05% at an illuminance of 294 lux, an exposure time of 5.6 lux, and 0 moving speed. The recall was unable to reach 100% because, in almost all data of the experiment set results, QR codes identification failed at rotations of 40°, 50°, 130°, 140°, 220°, 230°, 310°, and 320°. In general, assume that the QR codes with those rotations (8 of 38 rotations) always failed to be identified, and the others would always be successfully identified in an ideal condition using the ZBar algorithm. The recall for that assumption was 78.95%. The maximum recall value obtained in the experiments in this paper was very close with the ideal maximum recall value of ZBar algorithm, also with the identification success rate of about 78.3% in upright QR codes, rotated QR codes, and irregular illumination conditions reported by Szentandrasi *et al.* [18].

The relationship of the recall of QR codes identification system with exposure and motion blur analyzed using non-linear regression analysis with robust base library on R. The optimization only needs data with high recall, so the data used in this paper only limited to the range of exposure of 1.0 lux·s - 3.5 lux·s and motion blur of 0.0 pixel - 4.0 pixel. The basis of the chosen upper boundary value of the exposure was the regression modeling of Fig. 13 would discontinue in the range between 3.5 lux·s and 4.0 lux·s. So, the upper boundary value of the exposure is chosen at 3.5 lux·s. The recall at 3.5 lux·s

was at about 60%. So, the lower boundary value of the exposure, the lower and upper boundary values of the motion blur chosen at the point near recall of 60%. We used the data within that boundary values for the analysis, and we assumed that the recall would be lower than 60% outside that boundary values.

TABLE II
EQUATIONS MODELS OF THE NON-LINEAR REGRESSION ANALYSIS OF RECALL AGAINST EXPOSURE WITH NO MOTION BLUR AND ITS RELATIVE GOODNESS-OF-FIT SCORE

Name	Equation	AICc Score	BIC Score
5th order polynomials	$r = \sum_{i=0}^{5} w_i H^i$	-138.5	-138.0
6th order polynomials	$r = \sum_{i=0}^{6} w_i H^i$	-151.7	-152.9
7th order polynomials	$r = \sum_{i=0}^{7} w_i H^i$	-146.4	-150.0
8th order polynomials	$r = \sum_{i=0}^{8} w_i H^i$	-139.9	-146.9
Exponential A	$r = k + (H - c) \cdot \exp(a + b \cdot H)$	-151.3	-149.2
Exponential B	$r = k + (H - c)^d \cdot \exp(a + b \cdot H)$	-167.0	-165.4

TABLE III
EQUATIONS MODELS OF THE NON-LINEAR REGRESSION ANALYSIS OF RECALL AGAINST MOTION BLUR AT CONSTANT EXPOSURE (1.63±0.03 LUX·S) AND ITS RELATIVE GOODNESS-OF-FIT SCORE

Name	Equation	AICc Score	BIC Score
2nd order polynomials	$r = \sum_{i=0}^{2} w_i MB^i$	-15.9	-36.1
3rd order polynomials	$r = \sum_{i=0}^{3} w_i MB^i$	20.6	-39.6
Gaussian-like	$r = x \cdot \left(\frac{-MB^2}{2y^2}\right)$	-10.5	-18.7
Exponential	$r = w - \exp(x + y \cdot MB)$	-30.1	-50.3

Predicting the regression equation model that could fit the data of recall against exposure and motion blur directly was hard. Our strategy was breaking down the regression analysis into three steps. The first and second steps were performing a regression analysis of recall against exposure with no motion blur and performing a regression analysis of recall against motion blur with a constant exposure value on the highest recall value (i.e., 1.63±0.03 lux·s). Both were only needed to find the equation model, which was the best to construct the non-linear regression equation of recall against exposure and motion blur. AICc (Akaike's Information Criterion for small samples) and BIC (Bayesian Information Criterion) Dziak *et al.* [31] used as the criteria to choose which equation model was having the best goodness-of-fit against the others, the lower of the value of them was the better. The equations modeled using polynomials and exponentials equation models. Table 2 showing that the best equation model that fits the recall against exposure with no motion blur data was "Exponential B". The best equation model that fits the recall against motion blur with a constant exposure on the highest recall value (i.e., 1.63±0.03 lux·s) data was "Exponential", as seen in Table 3.

TABLE IV
EQUATIONS MODELS OF THE NON-LINEAR REGRESSION ANALYSIS OF RECALL AGAINST EXPOSURE AND MOTION BLUR

Name	Equation	AICc Score	BIC Score
Fit 0	$r = o + (H - c)^d \cdot \exp(a + b \cdot H) - \exp(x + y \cdot MB)$	842.0	854.4
Fit 1	$r = (k + (H - c)^d \cdot \exp(a + b \cdot H)) \cdot (w - \exp(x + y \cdot MB))$	778.5	791.6
Fit 2	$r = o - k \cdot \exp(x + y \cdot MB) + w \cdot (H - c)^d \cdot \exp(a + b \cdot H + y \cdot MB)$	65.2	79.3
Fit 3	$r = o - k \cdot \exp(x + y \cdot MB) - (H - c)^d \cdot \exp(n + b \cdot H + y \cdot MB)$	447.0	460.1
Fit 4	$R = o + w \cdot (H - c)^d \cdot \exp(a + b \cdot H) - (H - c)^d \cdot \exp(n + b \cdot H + y \cdot MB)$	6.0	19.1
Fit 5	$r = o - (H - c)^d \cdot \exp(n + b \cdot H + y \cdot MB)$	482.6	494.2

TABLE V
REGRESSION CONSTANTS OF REGRESSION EQUATION "FIT 4"

Weight	Value
a	4.18046
b	-3.65950
c	1.05862
d	2.27629
n	-3.27108
o	0.60108
w	3.08732
y	2.18807

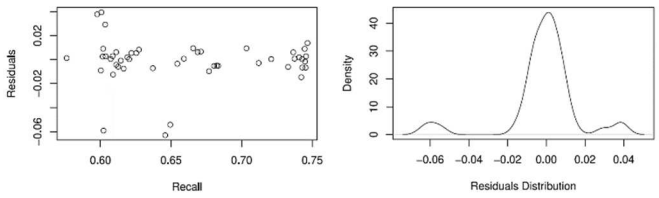

Fig. 14 Residual plot and normal residual plot of regression result "Fit 4", respectively

The last step was performing a regression analysis of recall against exposure and motion blur. We obtained the equation model by conducting binary operations (e.g., summation, multiply) between the equation models found on the first and second steps. Table 4 showed the equation "Fit 4" much better than the others. AICc and BIC are relative goodness-of-fit criteria so that they could not be used to measure whether the regression result has absolute goodness-of-fit. We assumed that the residual of the regression was normally distributed, homoscedastic, and unbiased. A normal residual plot used to check whether the residual of a regression result is normally distributed. A residual plot used to check the variance and the bias of the regression residual. From Fig. 14, it was known

that the regression result "Fit 4" had a normally distributed residual, the same variance of the residual (homoscedastic), and the residual had a 0-mean value (unbiased). From the residual plot, the residual of the regression result "Fit 4" was less than 2%, and it was relatively low when compared to the recall values so that the regression result was acceptable.

The regression weights of "Fit 4" had been obtained from the regression analysis result of the recall against exposure and motion blur, as seen in Table 5. We obtained the relationship of the recall against illuminance, exposure time, and moving speed by substituting the non-linear regression equation of recall against exposure and motion blur with its regression weights, that is

$$r = 0.60108 + (3.08732 \cdot (E \cdot t - 1.05862)^{2.27630} \cdot exp(4.18046 - 3.65951 \cdot E \cdot t)) - ((E \cdot t - 1.05862)^{2.27630} \cdot exp(-3.27108 - 3.65951 \cdot E \cdot t + 2.18807 \cdot v \cdot t \cdot \frac{n_m}{FOV_m})) \quad (8)$$

hence the equation could be used to optimize illuminance and exposure time in various moving speeds to maximize the recall.

B. *The optimum illuminance and exposure time in various moving speeds*

The optimization process follows E and t optimization methods that had already explained in Section II-B-3 using data given in Section III-A. The optimization focused on improving the recall because the precision had already always been 100%. The maximum possible recall was 74.72%, but it was rounded to 74.5% to make the scale of the charts more comfortable to read. The r_{tol} of 0.1% used in the optimization process and rtol of 5% used for drawing charts.

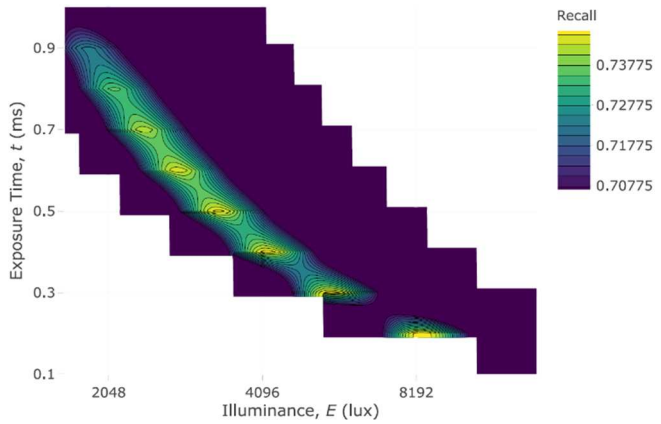

Fig. 15 Recalls against various illuminance and exposure time at 2.5 m/s

Fig. 15 shows an example chart of the recalls against various illuminance and exposure time for a moving speed of 2.5 m/s. There might be some multiple illuminance and exposure time sets that give nearly the same recall from the generated charts. The best decision was to choose set with lower illuminance as long as the recall did not less than the chosen tolerance.

We calculated the optimum illuminance and exposure time for relative moving speeds 0 m/s - 2.5 m/s. We also calculated for higher relative moving speeds up to 15 m/s, as seen in Fig. 16. It was possible to calculate the optimum illuminance and exposure time for moving speed beyond 15 m/s, as long as it was still within our data boundaries of the experiment results in terms of exposure and motion blur. From Fig. 16, it could be seen that the exposure time reduced to keep the motion blur low as the moving speed increased, but more illuminance was needed to keep the image well-exposed so that the recall kept maximum. The exposure time value and illuminance value should be optimum; otherwise, the recall decreased, as seen in Fig. 16, where the recall starts decreasing at 7.8 m/s because of motion blur. It is limited by the specification t_{min} and t_{step} of the camera.

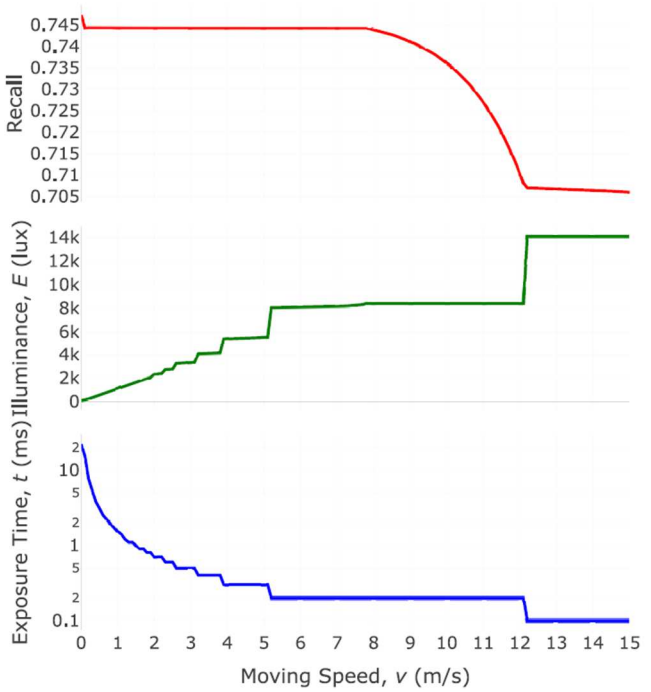

Fig. 16 The optimum E and t and its recall (precision always 100%) for the given range of speed for QR codes identification system in this paper

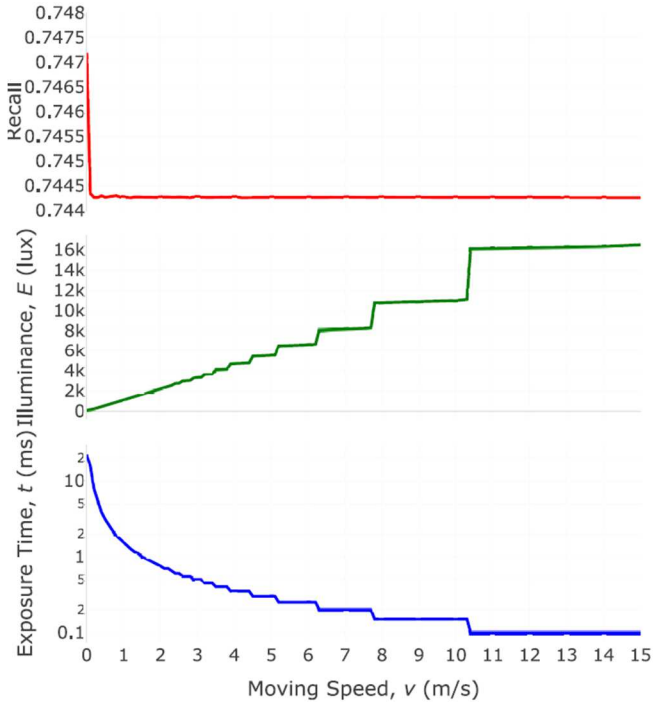

Fig. 17 The optimum E and t and its recall (precision always 100%) for a given range of speed for QR codes identification system with lower minimum and step of exposure time

For example, if the imaging system replaced with the same camera but different on t_{min} and t_{step} that was 0.05 ms both, then the system's recall be able to be kept at maximum even beyond 7.8 m/s (as seen in Fig. 17). At some point in the moving speed, the recall might decrease again, but it was possible to keep maximum recall again as long as there was a camera with lower minimum exposure time and exposure time step.

C. Applications

The approach in this work might be applied in the QR code indoor localization and navigation system for mobile robots [1] to maximize QR code identification performance. The quantitative value of the camera exposure time and the illuminance on the QR code to be used for that system for the required moving speed able to obtain. In that case, the mobile robot moving speed was 2.5 m/s, and it is covered experimentally within this work. Zhang *et al.* [1] also used the ZBar algorithm for QR code identification. The possible values for camera exposure time and the illuminance on the QR code are available to obtain by drawing a graph using Equation 8 for a given moving speed, camera FOV on the moving direction, and image resolution on the moving direction.

The smart wheelchair with QR codes localization system in Cavanini *et al.* [8] can be improved using the approach in this work to address possible future problems when the smart wheelchair is used in real-life scenarios. Commonly known in real life, wheelchair usage is to move someone who is using it. We open the possibilities for the smart wheelchair in Cavanini *et al* [8] to maximize QR code identification performance while moving.

Systems other than the localization system that require moving QR code identification performance are also possible to apply the approach in this work, such as vision-based structural displacement measurement [10]. The displacements of the QR codes were done by vibration process using a shaking table with a particular vibration frequency. Our approach in this work was using linear moving speed. It is possible to derive linear moving speed into the vibration frequency since the displacements measured linearly.

IV. Conclusion

This study analyzed the root cause of low identification performance on the Quick Response (QR) codes identification system. The study case on the ZBar algorithm showed that illuminance, exposure time, and moving speed affect QR codes identification system performance. Illuminance and exposure time affect images exposure that could make the image under-exposed or over-exposed; hence the contrast of the QR codes decreased so that the identification failed. The exposure time itself could make a motion blur on the image if the QR codes were moving; hence the structure of the QR codes was blurred, distorted, and overlapping with each other so that the identification failed. The relationship of the recall and the precision of the QR codes identification system against illuminance, exposure time, and moving speed was analyzed and represented with a non-linear regression equation. We also proposed a novel solution to overcome the physical phenomena that made QR codes identification system performance low by optimizing the illuminance and exposure time of the system for certain required moving speeds; hence, the identification performance maximized. The optimization performed using the numerical method presented in this paper. The optimization process started with specifying the requirements and the specifications of the system, then calculating boundaries, generating illuminance and exposure time values sets, calculating system identification performance for each value set, and setting the selection with a given criterion. The study case also showed that this method effectively maximizes the performance of the system of moving QR codes identification, even on higher moving speeds up to 2.5 m/s. Our calculations were valid, as its still within exposure and motion blur boundaries set by our experiment result data.

Nomenclature

d	distance	m
E	illuminance on an object	lux
f	focal length	m
FN	false negatives count	-
FP	false positives count	-
FOV	field of view	m
H	exposure	lux·s
MB	motion blur	pixel
n	image resolution (pixels count)	pixel
p	precision	-
r	recall	-
s	length on a particular direction	m
t	camera exposure time	s
TP	true positives count	-
TN	true negatives count	-
v	relative moving speed	ms^{-1}

Subscripts

ob	between the camera and QR code
lens	camera lens
m	on the moving direction of the objects
max	maximum
min	minimum
sensor	camera sensor
tol	tolerance

Acknowledgment

The authors are grateful for the research support by the Faculty of Engineering, Universitas Gadjah Mada.

References

[1] H. Zhang, C. Zhang, W. Yang, and C.-Y. Chen, "Localization and navigation using QR code for mobile robot in indoor environment," in *2015 IEEE International Conference on Robotics and Biomimetics (ROBIO)*, Dec. 2015, pp. 2501–2506, doi: 10.1109/ROBIO.2015.7419715.

[2] R. Taketani and H. Kobayashi, "A Proposal for Improving Estimation Accuracy of Localization Using QR codes and Image Sensors," in *IECON Proceedings (Industrial Electronics Conference)*, Oct. 2019, vol. 2019-Octob, pp. 6815–6820, doi: 10.1109/IECON.2019.8927589.

[3] Z. Li and J. Huang, "Study on the use of Q-R codes as landmarks for indoor positioning: Preliminary results," in *2018 IEEE/ION Position, Location and Navigation Symposium (PLANS)*, Apr. 2018, pp. 1270–1276, doi: 10.1109/PLANS.2018.8373516.

[4] P. Nazemzadeh, D. Fontanelli, D. Macii, and L. Palopoli, "Indoor Localization of Mobile Robots Through QR Code Detection and Dead Reckoning Data Fusion," *IEEE/ASME Trans. Mechatronics*, vol. 22,

no. 6, pp. 2588–2599, Dec. 2017, doi: 10.1109/TMECH.2017.2762598.

[5] J. Tang, W. Zhu, and Y. Bi, "A Computer Vision-Based Navigation and Localization Method for Station-Moving Aircraft Transport Platform with Dual Cameras," *Sensors*, vol. 20, no. 1, p. 279, Jan. 2020, doi: 10.3390/s20010279.

[6] N. T. Truc and Y.-T. Kim, "Navigation Method of the Transportation Robot Using Fuzzy Line Tracking and QR Code Recognition," *Int. J. Humanoid Robot.*, vol. 14, no. 02, p. 1650027, Jun. 2017, doi: 10.1142/S0219843616500274.

[7] A. S. Maner, D. Devasthale, V. Sonar, and R. Krishnamurti, "Mobile AR System using QR Code as Marker for EHV Substation Operation Management," in *2018 20th National Power Systems Conference (NPSC)*, Dec. 2018, pp. 1–5, doi: 10.1109/NPSC.2018.8771834.

[8] L. Cavanini *et al.*, "A QR-code localization system for mobile robots: Application to smart wheelchairs," in *2017 European Conference on Mobile Robots (ECMR)*, Sep. 2017, pp. 1–6, doi: 10.1109/ECMR.2017.8098667.

[9] Y. Mashiba, H. E. B. Salih, N. Wakatsuki, K. Mizutani, and K. Zempo, "QR code without impairing the scenery and detection system for the visually impaired," in *2020 IEEE 9th Global Conference on Consumer Electronics, GCCE 2020*, Oct. 2020, pp. 888–892, doi: 10.1109/GCCE50665.2020.9291733.

[10] X. W. Ye, T. H. Yi, C. Z. Dong, and T. Liu, "Vision-based structural displacement measurement: System performance evaluation and influence factor analysis," *Meas. J. Int. Meas. Confed.*, vol. 88, pp. 372–384, 2016, doi: 10.1016/j.measurement.2016.01.024.

[11] J. Qian, X. Du, B. Zhang, B. Fan, and X. Yang, "Optimization of QR code readability in movement state using response surface methodology for implementing continuous chain traceability," *Comput. Electron. Agric.*, vol. 139, pp. 56–64, Jun. 2017, doi: 10.1016/j.compag.2017.05.009.

[12] K. Liang *et al.*, "Development and parameter optimization of automatic separation and identification equipment for grain tracing systems based on grain tracers with QR codes," *Comput. Electron. Agric.*, vol. 162, no. March, pp. 709–718, 2019, doi: 10.1016/j.compag.2019.04.039.

[13] D. Mourtzis, V. Samothrakis, V. Zogopoulos, and E. Vlachou, "Warehouse Design and Operation using Augmented Reality technology: A Papermaking Industry Case Study," *Procedia CIRP*, vol. 79, pp. 574–579, 2019, doi: 10.1016/j.procir.2019.02.097.

[14] X. Yu *et al.*, "Positioning, Navigation, and Book Accessing/Returning in an Autonomous Library Robot using Integrated Binocular Vision and QR Code Identification Systems," *Sensors*, vol. 19, no. 4, p. 783, Feb. 2019, doi: 10.3390/s19040783.

[15] H. Li, T. Chen, Y. Peng, and H. Li, "An intelligent vehicle-tracking system solution for indoor parking," *Appl. Geomatics*, vol. 12, no. 4, pp. 481–490, Dec. 2020, doi: 10.1007/s12518-020-00321-8.

[16] W. Hogpracha and S. Vongpradhip, "Recognition system for QR code on moving car," in *10th International Conference on Computer Science and Education, ICCSE 2015*, 2015, no. Iccse, pp. 14–18, doi: 10.1109/ICCSE.2015.7250210.

[17] J. Brown, "ZBar bar code reader," 2010.

[18] I. Szentandrási, A. Herout, and M. Dubská, "Fast detection and recognition of QR codes in high-resolution images," in *Proceedings of the 28th Spring Conference on Computer Graphics - SCCG '12*, 2012, vol. 1, no. 212, pp. 129–136, doi: 10.1145/2448531.2448548.

[19] Y. Liu, J. Yang, and M. Liu, "Recognition of QR Code with mobile phones," in *2008 Chinese Control and Decision Conference*, Jul. 2008, pp. 203–206, doi: 10.1109/CCDC.2008.4597299.

[20] Y. He and Y. Yang, "An Improved Sauvola Approach on QR Code Image Binarization," in *2019 IEEE 11th International Conference on Advanced Infocomm Technology, ICAIT 2019*, Oct. 2019, pp. 6–10, doi: 10.1109/ICAIT.2019.8935907.

[21] H. Pu, M. Fan, J. Yang, and J. Lian, "Quick response barcode deblurring via doubly convolutional neural network," *Multimed. Tools Appl.*, vol. 78, no. 1, pp. 897–912, Jan. 2019, doi: 10.1007/s11042-018-5802-2.

[22] X. Yu and W. Xie, "Real-time recovery and recognition of motion blurry QR code image based on fractional order deblurring method," *IET Image Process.*, vol. 13, no. 6, pp. 923–930, May 2019, doi: 10.1049/iet-ipr.2018.5792.

[23] S. Yu, "Learning from giving peer feedback on postgraduate theses: Voices from Master's students in the Macau EFL context," *Assess. Writ.*, vol. 40, pp. 42–52, 2019, doi: 10.1016/j.asw.2019.03.004.

[24] I. Jahr, "Lighting in Machine Vision," in *Handbook of Machine and Computer Vision*, Weinheim, Germany: Wiley-VCH Verlag GmbH & Co. KGaA, 2017, pp. 63–178.

[25] A. Godil, R. Bostelman, W. Shackleford, T. Hong, and M. Shneier, "Performance Metrics for Evaluating Object and Human Detection and Tracking Systems," Gaithersburg, MD, Jul. 2014. doi: 10.6028/NIST.IR.7972.

[26] H. Mattfeldt, "Camera Systems in Machine Vision," in *Handbook of Machine and Computer Vision*, Weinheim, Germany: Wiley-VCH Verlag GmbH & Co. KGaA, 2017, pp. 317–397.

[27] N. Holmes, "Camera Computer Interfaces," in *Handbook of Machine and Computer Vision*, Weinheim, Germany: Wiley-VCH Verlag GmbH & Co. KGaA, 2017, pp. 431–503.

[28] A. Rowlands, "Fundamental optical formulae," in *Physics of Digital Photography*, IOP Publishing, 2017, pp. 1–62.

[29] G. Patel and G. Panchal, "Quick response codes decodability improvements using error correction levels," in *2017 International Conference on Intelligent Sustainable Systems (ICISS)*, Dec. 2017, no. Iciss, pp. 231–234, doi: 10.1109/ISS1.2017.8389404.

[30] R. Petrella, M. Tursini, L. Peretti, and M. Zigliotto, "Speed measurement algorithms for low-resolution incremental encoder equipped drives: a comparative analysis," in *2007 International Aegean Conference on Electrical Machines and Power Electronics*, Sep. 2007, pp. 780–787, doi: 10.1109/ACEMP.2007.4510607.

[31] J. J. Dziak, D. L. Coffman, S. T. Lanza, R. Li, and L. S. Jermiin, "Sensitivity and specificity of information criteria," *Brief. Bioinform.*, vol. 21, no. 2, pp. 553–565, Mar. 2020, doi: 10.1093/bib/bbz016.